PSFC/JA-22-107

Robust Identification of Multiple Input Single Output System Response for Efficient Pickup Noise Removal from Tokamak Diagnostics

T. Odstrcil,[1] F. Laggner,[2] A. M. Rosenthal,[3] A. Bortolon,[2] J. Hughes,[3]
J. C. Spendlove,[4] and T. Wilks[3]

[1]General Atomics, San Diego, CA 92186-5608, USA
[2]Princeton Plasma Physics Laboratory, Princeton, NJ 08543, USA
[3]Massachusetts Institute of Technology, Cambridge, MA, 02139, USA
[4]Brigham Young University, Provo, UT 84602, USA

August 2022

Plasma Science and Fusion Center
Massachusetts Institute of Technology
Cambridge MA 02139 USA

This material is based upon work supported by the U.S. Department of Energy, Office of Science, Office of Fusion Energy Sciences, using the DIII-D National Fu- sion Facility, a DOE Office of Science user facility, un- der Award(s) DE-FC02-04ER54698, DE-SC0014264 and DE-AC02-09CH11466. Reproduction, translation, publication, use and disposal, in whole or in part, by or for the United States government is permitted.

Submitted to *Review of Scientific Instruments*

Robust Identification of Multiple Input Single Output System Response for Efficient Pickup Noise Removal from Tokamak Diagnostics

T. Odstrcil,[1, a)] F. Laggner,[2] A. M. Rosenthal,[3] A. Bortolon,[2] J. Hughes,[3] J. C. Spendlove,[4] and T. Wilks[3]
[1)] *General Atomics, San Diego, CA 92186-5608, USA*
[2)] *Princeton Plasma Physics Laboratory, Princeton, NJ 08543, USA*
[3)] *Massachusetts Institute of Technology, Cambridge, MA, 02139, USA*
[4)] *Brigham Young University, Provo, UT 84602, USA*

(Dated: 3 August 2022)

Electromagnetic pickup noise in the tokamak environment imposes an imminent challenge for measuring weak diagnostic photocurrents nA range. The diagnostic signal can be contaminated by an unknown mixture of crosstalk signals from coils powered by currents in kA range. To address this issue, an algorithm for robust identification of linear multi-input single-output (MISO) systems has been developed. MISO model describes the dynamic relationship between measured signals from power sources and observed signals in the diagnostics and allows for a precise subtraction of the noise component. The proposed method was tested on experimental diagnostic data from the DIII-D tokamak, and it has reduced noise by up to 20 dB in 1–20 kHz range.

I. INTRODUCTION

The operation of plasma diagnostics in tokamaks presents many challenges. Take for example measurements of photocurrents from vacuum ultraviolet cameras of LLAMA[1] or soft X-ray diagnostics on DIII-D tokamak. Because the radiation at VUV and soft X-ray energies are readily absorbed in air, and optical components are inefficient, these two diagnostics are designed as pinhole cameras connected to a primary tokamak vacuum. Placing a diagnostic in the tokamak introduces challenges in terms of limited space, electromagnetic noise, and a harsh radioactive environment. Since the observed photocurrents are relatively small, in 10^{-9} A range, despite the best effort for electromagnetic shielding, the crosstalk with surrounding poloidal field coils can contaminate the measured signal. The shaping coils are powered by independently controlled high-voltage power sources and choppers producing a high-frequency spike noise. Although the chopper voltages and coil currents are digitized, the noise cannot be reliably removed without an accurate model for crosstalk.

We will assume that the crosstalk can be characterized by a causal linear time-invariant (LTI) multiple-input, single-output (MISO) model. The MISO model identification is commonly used in a wide range of applications, for example; body dynamics[3], analysis of neuron activity[4] or modeling of complex chemical processes[5]. This study aims to develop a robust and efficient algorithm for the identification of the MISO model determining the dynamic relation between noise signals and measured output signals from the diagnostic. The identified model then provides a prediction of the noise signal, which can be subtracted from the measured output to recover the original plasma signal.

[a)] Electronic mail:odstrcilt@fusion.gat.com

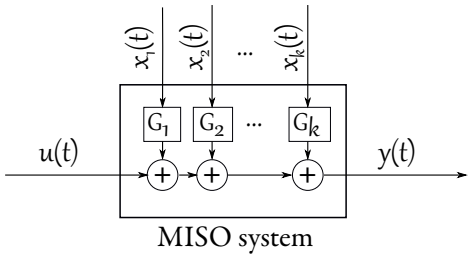

FIG. 1. Schematic representation of MISO system with k inputs $x_i(t)$ filtered by transfer functions G_i, output $y(t)$ and plasma signal $u(t)$.

II. ALGORITHM FOR MISO IDENTIFICATION

The MISO system is illustrated in Fig. 1, where photocurrent $u(t)$ is mixed with k input noise signals $x_i(t)$, modified by unknown transfer functions G_i, producing the measured output signal $y(t)$. There are several common options for the description of the MISO systems[6?] . We have used the nonparametric finite impulse response (FIR) model because FIR models are estimated directly from input-output signals by the linear least-squares method. Additionally, with sufficiently high order, FIR models can approximate any LTI system.

Consider a MISO system represented by a bank of k FIR filters $h_i[m]$ with memory length N. Let $x_i[m]$, for $i \in \{1, \ldots, k\}$, be the measured discrete time inputs of length n, $y[m]$ be the measured output and the $u[m]$ be the unmeasured plasma signal. Then, equation

$$y[m] = \sum_{i=1}^{k} \sum_{\tau=0}^{N-1} h_i[\tau] x_i[m-\tau] + u[m], \qquad (1)$$

describes relation between MISO system input and outputs. In order to solve this problem, we need to assume that the signal $u[m]$ and the lagged signals $x_i[m-\tau]$ are uncorrelated. Limitation of this assumption will be discussed later in Sec. III B about the real diagnostic data.

The objective of the MISO identification algorithm is to provide the best estimate of discrete FIR coefficients $h_i[m]$ for each input signal. To simplify this problem, we assume that the signals x_i and y are periodic. If $n \gg N$, this assumption has a negligible effect on the final estimate of FIR coefficients. Then the Eq. (1) can be rewritten in the convenient form of a matrix equation

$$\mathbf{y} = \mathbb{X}\mathbf{h} + \mathbf{u} \tag{2}$$

where $\mathbf{y} \in R^n$ and $\mathbf{u} \in R^n$ are vectors with the measured output and plasma signal. The vector $\mathbf{h} \in R^{kN}$ consists of concatenated FIR coefficients

$$\mathbf{h} = (h_1[0], \ldots, h_1[N], \ldots, h_k[0], \ldots, h_k[N])^T \tag{3}$$

and matrix $\mathbb{X} \in R^{kN,n}$ is a block matrix

$$\mathbb{X} = [\mathbb{X}_1, \ldots, \mathbb{X}_k], \tag{4}$$

where $\mathbb{X}_\mathbb{k} \in R^{N,n}$ is a lag matrix of signal x_k

$$\mathbb{X}_\mathbb{k} = \begin{pmatrix} x_k[1] & x_k[n] & \cdots & x_k[n-N+2] \\ x_k[2] & x_k[1] & \cdots & x_k[n-N+3] \\ \vdots & \vdots & \ddots & \vdots \\ x_k[n] & x_k[n-1] & \cdots & x_k[n-N+1] \end{pmatrix}$$

Since u is assumed to be uncorrelated with all lagged $x_i[n]$ signals, vector $\mathbf{u}$ is part of the orthogonal complement of linear space spanned by columns of $\mathbb{X}$, and thus the unbiased estimate of $\mathbf{h}$ is provided by least squares

$$\hat{\mathbf{h}} = \underset{h}{\operatorname{argmin}} ||\mathbf{y} - \mathbb{X}\mathbf{h}||_2^2 \tag{5}$$

However, this approach has two drawbacks. First, if the signals x_k are correlated in time (i.e., they are represented by a highly colored noise) or if they are correlated in between each other, the least-squares problem will be ill-posed, and a random variance will dominate estimate in h_i coefficients. The second issue is that the standard methods for least-squares are based on QR or SVD[7], and calculation can become unacceptably slow for expected matrix $\mathbb{X}$ size of about $10^4 \times 10^6$ coefficients.

A. Regularised Least-Squares

Conditionality of the linear regression problem in Eq. (2) can be improved by adding *a priori* information about h_i coefficients. The objective function $\Lambda(\mathbf{h}, \lambda)$ of regularized least-squares method is

$$\Lambda(\mathbf{h}, \lambda) = ||\mathbf{y} - \mathbb{X}\mathbf{h}||_2^2 + \lambda||\mathbb{P}\mathbf{h}||_2^2 \tag{6}$$

where $\mathbb{P} \in R^{kN,kN}$ is penalty matrix for estimator of $\mathbf{h}$ and λ is regularization coefficient. By taking a first derivative of $\Lambda(\mathbf{h}, \lambda)$ with respect to $\mathbf{h}$ and equating it to zero, one obtains following analytical expression for estimate of $\mathbf{h}$

$$\hat{\mathbf{h}}(\lambda) = \left(\mathbb{X}^T\mathbb{X} + \lambda\mathbb{P}^T\mathbb{P}\right)^{-1}\mathbb{X}^T\mathbf{y}. \tag{7}$$

Vector $\phi_{x_k y} \equiv \frac{1}{n}\mathbb{X}^T\mathbf{y}$ expresses cross-correlations between $\mathbf{y}$ and lagged $\mathbf{x}_k$ vectors. Further, $\Phi_{xx} \equiv \frac{1}{n}\mathbb{X}^T\mathbb{X}$ is a block matrix of auto- and cross-correlations[3,4] $\Phi_{x_i x_j}(i,j) = \phi_{x_i x_j}(i-j)$. Exploiting the regular Toeplitz structure of each $\Phi_{x_i x_j}$ matrix, the multiplication complexity of $\mathbb{X}^T\mathbb{X}$ is reduced N-times compared to a naive implementation.

If one chooses $\mathbb{P}$ to be the identity matrix, the objective function will minimize the Euclidean norm of $\hat{\mathbf{h}}$. Such case is referred as Ridge regression[8] (RR). Another common choice for $\mathbb{P}$ is the first difference matrix minimizing the unsmoothness of the FIR function. This case is referred as Tikhonov-Phillips regularization[9] (TPR). Because the variation in FIR coefficients of the overdamped system is decreasing with lag index, we can multiply the first difference matrix $\mathbb{D} \in R^{N,N}$ by linearly increasing weight[5] to improve the performance

$$\mathbb{D} = \begin{pmatrix} 1 & -1 & 0 & \cdots & 0 & 0 \\ 0 & 2 & -2 & \cdots & 0 & 0 \\ \vdots & \vdots & \vdots & \ddots & \vdots & \vdots \\ 0 & 0 & & \cdots & 0 & N \end{pmatrix},$$

and the penalty matrix $\mathbb{P}$ is defined as a block matrix with k matrices $\mathbb{D}$ on the diagonal.

Efficient method for solution of Eq. 7 is provided by eigenvalue decomposition of symmetric and positive definite matrix $\tilde{\mathbb{X}}^T\tilde{\mathbb{X}}$, where $\tilde{\mathbb{X}} = \mathbb{X}\mathbb{P}^{-1}$

$$\mathbb{Q}\mathbb{\Lambda}\mathbb{Q}^T = \tilde{\mathbb{X}}^T\tilde{\mathbb{X}}. \tag{8}$$

$\mathbb{\Lambda}$ is a diagonal matrix of eigenvalues, i.e. $\Lambda_{ii} = \lambda_i$ and columns of orthonormal matrix $\mathbb{Q}$ are corresponding eigen-vectors. The solution of Eq. (7) is expressed as

$$\hat{\mathbf{h}}(\lambda) = \tilde{\mathbb{Q}}\left(\mathbb{\Lambda} + \lambda\mathbb{I}\right)^{-1}\tilde{\mathbb{Q}}\mathbb{X}^T\mathbf{y} \tag{9}$$

where $\tilde{\mathbb{Q}} = \mathbb{P}^{-1}\mathbb{Q}$. Evaluation of $\tilde{\mathbb{Q}}$ and $\tilde{\mathbb{X}}^T\tilde{\mathbb{X}}$ can be done efficiently by taking advantage of bi-diagonal pattern of $\mathbb{P}$ matrix[10]. The rest of Eq. (9) involves only a matrix multiplication and a trivial inversion of the diagonal matrix. The computational time of the algorithm is dominated by the eigenvalue decomposition with $\mathcal{O}(k^3N^3)$, and evaluation of correlations for $\mathbb{X}^T\mathbb{X}$ with $\mathcal{O}(nNk^2)$ complexity.

B. Selection criterion

The last remaining step is a selection of the regularization coefficient λ, which modifies the balance between random variance error and bias introduced by the regularization. A promising result provides generalized cross-validation (GCV). Although this method was originally proposed as λ estimator for RR[11], it can be generalized for arbitrary penalty matrix[12]. GCV is a rotation-invariant analytical approximation of basic one-leave-out cross-validation. GCV estimate of λ is the minimizer of $V(\lambda)$ given by[11]

$$V(\lambda) = \frac{1}{n}||(\mathbb{I} - \mathbb{A}(\lambda)y)||_2^2 \Big/ \left[\frac{1}{n}\mathrm{Tr}(\mathbb{I} - \mathbb{A}(\lambda))\right]^2, \tag{10}$$

where matrix $\mathbb{A}(\lambda)$ is defined by a relation $\mathbb{X}\hat{\mathbb{h}}(\lambda) = \mathbb{A}(\lambda)\mathbb{y}$. Using the eigenvalue decomposition in Eq. (8), one can express GCV in a more pragmatic form

$$V(\lambda) = \frac{\frac{1}{n}\left[\sum_{i=0}^{kN}\left(\frac{\lambda/\sqrt{\lambda_i}}{\lambda+\lambda_i}(\tilde{\mathbb{Q}}\mathbb{X}^T\mathbf{y})_i\right)^2 + ||\mathbf{y}_\perp||_2^2\right]}{\frac{1}{n^2}\left(\sum_{i=1}^{kN}\frac{\lambda}{\lambda+\lambda_i} + n - kN\right)^2}. \quad (11)$$

The vector $\mathbf{y}_\perp$ is projection of $\mathbf{y}$ onto the orthogonal complement of $\mathbb{X}$ calculated as $\mathbf{y}_\perp = (\mathbb{I}-\mathbb{X})\hat{\mathbf{h}}(0)$. This form of $V(\lambda)$ is advantagous for optimisation because once $\tilde{\mathbb{Q}}\mathbb{X}^T\mathbf{y}$ and $\mathbf{y}_\perp$ are evaluated, the rest of the expression for $V(\lambda)$ has the computational complexity of mere $\mathcal{O}(Nk)$.

III. NOISE REMOVAL FROM LLAMA DIAGNOSTIC

LLAMA[1] (**L**yman **A**lpha **M**easurement **A**pparatus) is a 1D pinhole camera installed on DIII-D tokamak to measure the Ly-α hydrogen neutral line at 121.6 nm. The diagnostic is absolutely calibrated[13] and measures the Ly-α brightness at 40 lines of sight. The camera views are centered near the separatrix below the midplane, with one-half of the channels observing the high-field side (HFS) and the other half observing the low-field side (LFS) of the plasma. Radiation is detected by two AXUV photodiode arrays consisting of 20 photodiodes with a common ground. AXUV arrays are connected via short shielded wires to vacuum feedthrough. The photocurrents are amplified with variable gain 10^7–10^8 V/A integrated circuit amplifiers, mounted directly to the airside of the vacuum flange to minimize the length of cables and a common pickup. The amplified signals are further converted to pseudo-differential signals that are less susceptible to noise and digitized outside the DIII-D machine hall. The LLAMA signals are digitized at 0.5 MHz rate; however, the frequency response is limited by the amplifier's 10 kHz cut-off frequency. Therefore, the signals are downsampled to 40 kHz before further processing to reduce their size.

A. MISO Identification of Artificial LLAMA Model

The algorithm described above has been validated first on artificial data set. The rationale behind the use of artificial data is that the system response and inputs are known exactly. This allows us to characterize the algorithm's performance and understand its behavior when all the assumptions are fulfilled.

The inputs x_k are generated using $k = 65$ normally distributed independent white noise sources with $n = 320000$ samples, mimicking 8 s of LLAMA signal downsampled to 40 kHz. All inputs were band-limited by 2nd order Butterworth filter at 40% of Nyquist rate. The output was determined by filtering input signals x_k independently by a digital Butterworth filter with random order in range

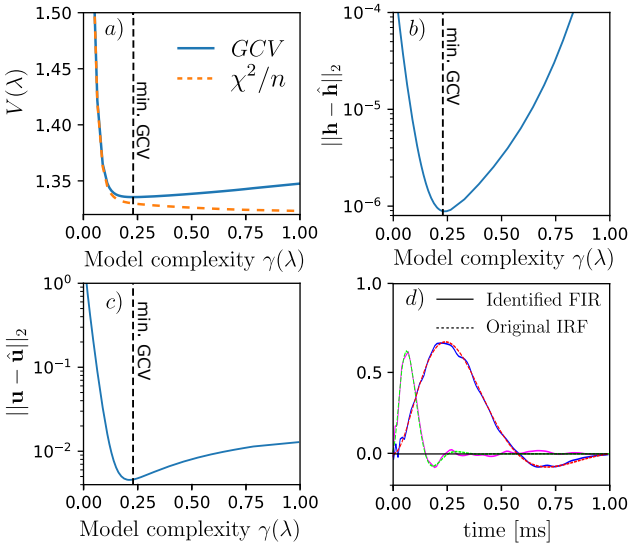

FIG. 2. Results of MISO identification of artificial data set illustrated by a) GCV estimator $V(\lambda)$ and denominator of Eq. (10) equal to χ^2/n, b) difference between estimated FIR $\hat{\mathbf{h}}$ and original IRF from Butterworth filters $\mathbf{h}$, c) difference between predicted plasma signal $\hat{\mathbf{u}}$ and original $\mathbf{u}$, d) examples of two FIR function (blue, magneta full line) $\hat{\mathbf{h}}(\lambda)$ evaluated at $V(\lambda)$ minimum and compared to original IRF (green, red, dashed line).

1–4 and random cut-off frequency ranging from 10% to 50% of Nyquist rate. Filtered input signals were then scaled by a random number in the range $(0, 1)$ and mixed together. At last, the artificial plasma signal u has been added. The amplitude of the plasma signal was set to 10% of noise, and it was filtered by 2nd order Butterworth filter with a cut-off at 50% of Nyquist frequency, matching the LLAMA amplifier cut-off at 10 kHz. The MISO model consists of a bank of k FIR filters with memory $N = 40$, describing 1 ms long impulse response functions (IRFs). Results of the model identification performed by the TPR method are presented in Fig. 2 as a function of the model complexity $\gamma(\lambda)$ defined by

$$\gamma(\lambda) = \frac{1}{kN}\sum_{i=1}^{kN}\frac{\lambda_i}{\lambda+\lambda_i}. \quad (12)$$

Parameter $\gamma(\lambda)$ describes the fraction of the largest eigenvalues λ_i contributing to the solution of Eq. (9). Therefore, the most complex model corresponding to unbiased least squares with $\lambda = 0$, has γ equal one, while the bias dominated model with λ approaching infinity has γ equal zero. The GCV estimator $V(\lambda)$ in Fig. 2a is relatively flat because $Nk \ll n$, however the $V(\lambda)$ minimum well estimates the optimal model complexity, minimizing the prediction error. The prediction error of FIR functions $\mathbf{h}$ in Fig. 2b has a steep dependence on the γ, because as more small eigen-values remains unbiased in Eq. (9), the random variance of the estimated FIR increases[14]. On contrary, the prediction error for plasma signal in Fig. 2c

only moderately increases with γ, because the smallest eigenvalues λ_i corresponding to the lowest singular values σ_i of $\mathbb{X}$, i.e. $\sigma_i^2 = \lambda_i$ and the associated eigenvectors are partially attenuated by the multiplication with matrix $\mathbb{X}$ in Eq. (2). The accuracy of the identification algorithm confirms Fig. 2d, where the two original IRFs are nearly exactly overlapped by identified FIRs.

B. MISO Identification of Experimental LLAMA Data

The algorithm performance has been evaluated on experimental LLAMA measurements in DIII-D discharge #180908. A complete list of all 53 used input signals $x_i(t)$ from choppers and high voltage sources powering the magnetic coils is presented in Tab. I. The input signals are resampled to 40 kHz and interpolated on the same time base as the LLAMA signals from −0.5 to 7.5 s. Because the low-frequency part of x_i signals can be correlated with the low-frequency component of the plasma signal $u(t)$, violating the basic assumption made in Sec. II, a 100 Hz high-pass filter is applied on all input signals x_i and measured LLAMA outputs y_j. The low-frequency part of the signal of y_i is added back to u_i after the noise subtraction.

TABLE I. List of pointnames used as filter inputs $x_i(t)$.

Source	number of units
HX choppers	16
X choppers	20
HV choppers	3
C-coil power supply	5
D-coil power supply	5
T-coil power supply	3
V-coil power supply	2
SPA I-coil power supply	12
SS power supply	6
BPS toroidal field power supply	2
EPS central solenoid power supply	1

Because the pickup noise observed in different channels of LLAMA diagnostics is highly correlated, we have assumed that a single regularization coefficient λ is sufficient to describe the optimal MISO model complexity for all channels. Estimate of FIR coefficients thus provides Eq. (9) after replacing single vector $\mathbf{y}$ by a matrix $\mathbb{Y}$ with columns corresponding to 40 stacked y_i signals. Additionally, the denominator of $V(\lambda)$ in Eq. (11) is averaged over all channels to improve robustness of GCV estimate.

Fig. 3 shows the results of MISO identification of the real LLAMA data. The optimal model complexity γ in Fig. 3a estimated by GCV is 0.14, lower than for synthetic data because of a significant correlation among input signals x_i. This value of γ also minimise u_i error in Fig. 3c, estimated as a sum of squares of $\mathbf{u}_i$ from regions

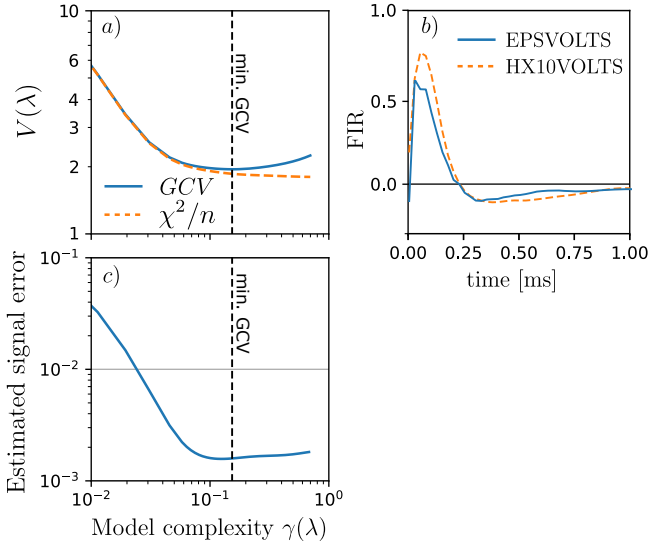

FIG. 3. Identification of MISO identification algorithm from the real LLAMA data; a) GCV estimator $V(\lambda)$ and denominator of Eq. (10) equal to χ^2/n b) example of estimated FIR functions from solenoid signal EPSVOLTS and poloidal field coils 6B chopper X10VOLTS, c) LLAMA signal error estimated from times before and after the discharge.

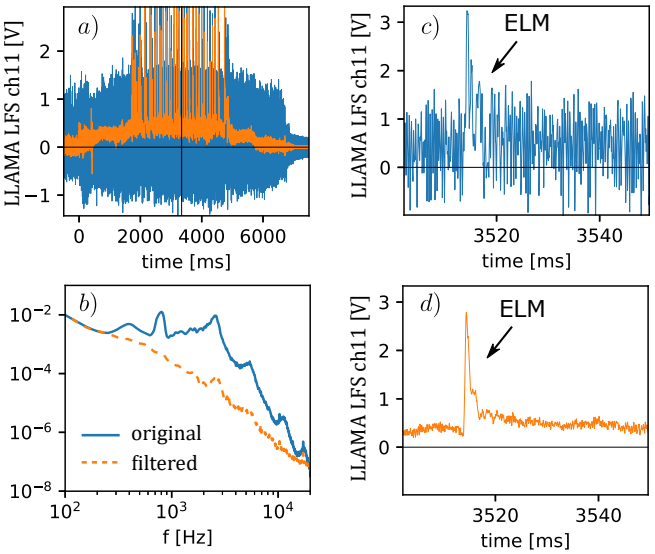

FIG. 4. Application of MISO model for noise removal in LLAMA data; a) original raw signal in blue, filtered in orange, b) power spectrum of the original and filtered signal, c) detail of a single ELM in the original signal, d) the same ELM after the noise subtraction.

before and after the discharge. As was already noted for the artificial model, the prediction error is weakly dependent on γ, and a higher model complexity does not significantly degrade the prediction accuracy of $\mathbf{u}_i$. Examples of FIR from the two largest noise sources are shown in Fig. 3b. The shape of the two FIR is similar because it is mainly determined by the transfer function of the LLAMA amplifier. However, they differ in details es-

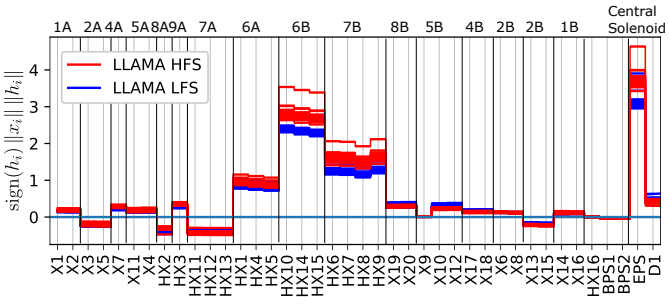

FIG. 5. Main contributions to the noise for all LLAMA channels. The upper labels indicate coil powered these sources.

sential for the accurate representation of the noise from these sources.

Results of the noise subtraction based on the identified MISO model are in Fig. 4. The amplitude of the pickup noise is reduced by a factor of 10 (20 dB) in the range between 1–10 kHz as shown in Fig. 4b. Moreover, the filter reveals fast ELM spike in Fig. 4d, without any loss in time resolution of the diagnostic. The same level of noise suppression was observed for all LLAMA channels. The last figure III B shows the contribution of the most important sources to the observed noise. The main contribution originates from poloidal field coils 6B, 7B, and 6A, nearest to LLAMA diagnostic and from the central solenoid. However, the contributions from the other coils are nonnegligible as well. Pickup noise is 15% higher in the HFS array, but relative contributions from different sources to both LLAMA arrays are nearly identical.

IV. CONCLUSION

In this paper, we have introduced the algorithm for identifying a model describing the dynamics of electromagnetic pickup noise propagation in tokamaks. The method is based on identifying the MISO model from an arbitrary number of inputs and one measured diagnostic signal contaminated by the noise. However, the underlying inversion problem is seriously ill-posed because the inputs are correlated and band-limited. Therefore, the TPR method is applied to identify a unique solution. The regularization level optimizing the bias-variance trade-off of the predicted signals provides GCV.

This algorithm was applied for a pickup noise removal from LLAMA diagnostic. After substraction, the observed noise was suppressed by 20 dB, corresponding to a factor of 10 reduction in the amplitude. The advantage of this method is that the time resolution of the diagnostics was not compromised, which is unavoidable if a low-pass filter is applied to eliminate the broadband noise. In addition, the algorithm provides information about the origins of pickup signals, useful for improving the electromagnetic shielding of the diagnostic. The application of this algorithm for other DIII-D diagnostics will be presented in future publications.

ACKNOWLEDGMENTS

This material is based upon work supported by the U.S. Department of Energy, Office of Science, Office of Fusion Energy Sciences, using the DIII-D National Fusion Facility, a DOE Office of Science user facility, under Award(s) DE-FC02-04ER54698, DE-SC0014264 and DE-AC02-09CH11466.

DATA AVAILABILITY STATEMENT

The data supporting this study's findings and the source code of the algorithm are available from the corresponding author upon reasonable request.

REFERENCES

[1] A. Rosenthal, J. Hughes, A. Bortolon, F. Laggner, T. Wilks, R. Vieira, R. Leccacorvi, E. Marmar, A. Nagy, C. Freeman, *et al.*, Review of Scientific Instruments **92**(3), 033523 (2021).
[2] E. Hollmann, L. Chousal, R. Fisher, R. Hernandez, G. Jackson, M. Lanctot, S. Pidcoe, J. Shankara, and D. Taussig, Review of Scientific Instruments **82**(11), 113507 (2011).
[3] E. J. Perreault, R. F. Kirsch, and A. M. Acosta, Biological cybernetics **80**(5), 327 (1999).
[4] D. T. Westwick, E. A. Pohlmeyer, S. A. Solla, L. E. Miller, and E. J. Perreault, Neural computation **18**(2), 329 (2006).
[5] B. S. Dayal and J. F. MacGregor, Industrial & engineering chemistry research **35**(11), 4078 (1996).
[6] J. Kasprzyk, IFAC Proceedings Volumes **42**(13), 278 (2009).
[7] G. H. Golub and C. F. Van Loan, *Matrix computations* (JHU press, 2013).
[8] A. E. Hoerl and R. W. Kennard, Technometrics **12**(1), 55 (1970).
[9] A. N. Tihonov, Soviet Math. **4**, 1035 (1963).
[10] W. H. Press, S. A. Teukolsky, W. T. Vetterling, and B. P. Flannery, *Numerical recipes 3rd edition: The art of scientific computing* (Cambridge university press, 2007).
[11] G. H. Golub, M. Heath, and G. Wahba, Technometrics **21**(2), 215 (1979).
[12] N. Terasaki, Y. Hosoda, M. Teranishi, and N. Iwama, Fusion engineering and design **34**, 801 (1997).
[13] F. Laggner, A. Bortolon, A. Rosenthal, T. Wilks, J. Hughes, C. Freeman, T. Golfinopoulos, A. Nagy, D. Mauzey, M. Shafer, *et al.*, Review of Scientific Instruments **92**(3), 033522 (2021).
[14] D. Westwick and R. E. Kearney, Medical and Biological Engineering and Computing **35**(2), 83 (1997).